Th1 polarization in *Bordetella pertussis* vaccine responses is maintained through a positive feedback loop

Lisa Willemsen[1], Jiyeun Lee[1], Pramod Shinde[1], Ferran Soldevila[1], Minori Aoki[1], Shelby Orfield[1], Mari Kojima[1], Ricardo da Silva Antunes[1], Alessandro Sette[1], Bjoern Peters[1,2,*]

[1] Center for Infectious Disease and Vaccine Research, La Jolla Institute for Immunology, La Jolla, CA, USA.
[2] Department of Medicine, University of California San Diego, La Jolla, CA, USA.
*Corresponding author: bpeters@lji.org

Abstract

Outbreaks of *Bordetella pertussis* (BP), the causative agent of whooping cough, continue despite broad vaccination coverage and have been increasing since vaccination switched from whole-BP (wP) to acellular BP (aP) vaccines. wP vaccination has been associated with more durable protective immunity and an induced Th1 polarized memory T cell response. Here, a multi-omics approach was applied to profile the immune response of 30 wP and 31 aP-primed individuals and identify correlates of T cell polarization before and after Tdap booster vaccination. We found that transcriptional changes indicating an interferon response on day 1 post-booster along with elevated plasma concentrations of IFN-γ and interferon-induced chemokines that peaked at day 1-3 post-booster correlated best with the Th1 polarization of the vaccine-induced memory T cell response on day 28. Our studies suggest that wP-primed individuals maintain their Th1 polarization through this early memory interferon response. This suggests that stimulating the interferon pathway during vaccination could be an effective strategy to elicit a predominant Th1 response in aP-primed individuals that protects better against infection.

Keywords: Vaccine, Bordetella pertussis, immune response, T cells, Th1 polarization.

Introduction

Whooping cough remains a significant and worldwide public health concern marked by periodic outbreaks and regularly life-threatening complications in young infants(1, 2). Whooping cough is caused by a respiratory infection with the *Bordetella pertussis* (BP) bacteria. In 1950, the initial vaccine, the alum-adjuvanted 'whole cell' (wP) inactivated BP vaccine, was administered and significantly reduced the disease incidence. However, due to adverse effects, the wP vaccine was replaced by an acellular pertussis (aP) vaccine. The aP vaccine contains different BP antigens including inactivated pertussis toxin (PT) and cell surface proteins of BP including filamentous hemagglutinin (FHA), fimbriae 2/3 (Fim2/3), and pertactin (PRN) and is administered together with tetanus toxoid (TT) and diphtheria toxoid (DT) as alum-adjuvanted DTaP vaccine to infants and as TdaP vaccine to teenagers and adults(3, 4). While the aP vaccine is generally associated with fewer adverse effects, the wP vaccine induces a broader and more robust immune response that lasts longer(5, 6). Interestingly, receipt of at least 1 wP dose significantly improves the durability of immunity despite subsequent aP doses as compared to exclusively aP priming and boosting(6). Although the aP vaccine protects against disease, it provides limited protection against infection compared to the wP vaccine which protects against both infection and disease(7, 8). The current resurgence of whooping cough has been linked to the switch to aP-priming(9-13). This resurgence may be explained by the distinct immune profiles elicited by these vaccines.

$CD4^+$ T cell immunity is required to protect against BP infection(3, 14). However, the type of T helper response between aP and wP-primed individuals differs and is each characterized by specific cytokine profiles and effector functions that coordinate immune responses to BP. Compared to wP vaccine priming, aP vaccine priming elicits a more Th2-polarized immune response(15-19) which is recognized by the production of interleukin-4 (IL-4), IL-5, IL-10, and IL-13 and associated with a humoral response including the production of IgE antibodies(20). Furthermore, Th2-polarized cells ensure the recruitment and activation of eosinophils and mast cells, thereby contributing to allergic inflammation(21). Compared to aP-primed individuals, wP-primed individuals show an increased Th1 over Th2-polarized immune response against BP which persists in adulthood despite aP booster vaccination(15-19). Th1-polarized cells primarily produce interferon-gamma (IFN-γ), tumor necrosis factor (TNF), and IL-2 and elicit both antibody-mediated and cell-mediated immunity(22). Th1 cells promote the phagocytosis and killing of pathogens by macrophages, enhance antigen presentation by dendritic cells, and stimulate the differentiation of cytotoxic T cells. Using a mouse model, research has shown that optimum protection against BP requires induction of a Th1, but not a Th2-polarized response(23). Additionally, natural infection with BP in children also induced a Th1-biased response(24).

T cell polarization starts with antigen-presenting cells (APC) presenting antigens via HLA-II to naive or memory T cells with a matching T cell receptor. This process can take place either at the local site of infection or vaccine administration or within the nearby draining lymph nodes. After antigen recognition and co-stimulation, APC secrete different cytokines which are the first triggers of T cell polarization. Researchers have described that IL-12(25-28) and IL-18(29) are

important Th1 polarizing cytokines, while IL-4 is known to stimulate Th2 polarization(30). The Th1 polarizing cytokines IL-12 and IL18 initiate the production of IFN-γ by NK and $CD8^+$ T cells within 2-6 hours after antigen exposure(31, 32). This early derived IFN-γ is essential for controlling certain infections before the remaining IFN-γ gets produced by other T cells. Early IFN-γ directly activates macrophages to enhance their capacity to eliminate pathogens but also regulates the differentiation of $CD4^+$ T cells into Th1 cells that will also start producing IFN-γ(33). Additionally, after booster vaccination or reinfection, IFN-γ will also be quickly produced by memory T cells which also contributes to Th1 polarization of naive T cells.

Previous research showed that BP infection is more severe in IFN-γ-depleted mice(34). Other researchers found that natural killer (NK) cell depletion caused disseminated lethal lung infection in BP-infected mice(35). This severe outcome was associated with a reduced antigen-specific Th1 response and increased Th2 response. Interestingly, Gillard et al. found that transcriptional antiviral responses on day 1 post-vaccination with Tdap-IPV (inactivated Poliovirus) were positively associated with antibody responses up to 1 year post-vaccination (36).

The mechanism of how wP-primed individuals maintain their Th1 polarization despite repeated aP boosters remains a puzzle(37). To identify factors contributing to increased Th1 polarization, we applied a multi-omics approach to profile the immune response of 31 aP and 30 wP-primed individuals longitudinally in the first 2 weeks post-vaccination and identified correlates of T cell polarization before and after TdaP booster vaccination. We confirmed the increased Th1 polarization in the wP individuals of our cohort and found that Th1-polarization pre-vaccination correlated positively with the vaccine-induced interferon response in PBMCs on day 1-3 post-booster on transcriptional and protein levels, which in turn correlated with a maintained Th1 polarization post-booster response. This suggested that changing the BP vaccination strategy by targeting the interferon pathway might boost Th1 responses against BP which could improve protection against infection and vaccine durability.

Results

Longitudinal samples from an adult cohort were collected to study TdaP booster vaccination-induced immune responses

We recruited healthy adults primed with either the aP (n=31) or wP (n=30) vaccine during infancy (**Figure 1A**). Study participants did not receive TdaP booster vaccinations four years prior to study enrollment and aP and wP groups were matched by sex (Table S1). From these participants, longitudinal blood samples were taken before (days -31, -14, and 0) and after TdaP booster vaccination (days 1, 3, 7, 14, and 28) (**Figure 1B**). The multiple pre-vaccination samples were utilized to establish robust baseline measurements per donor and were used to calculate post-booster responses. Previously, a multi-omics approach was applied to evaluate the immune response to BP vaccination by integrating plasma antigen-specific IgG levels including IgG isotypes (IgG1-4), plasma concentrations of 45 different cytokines, and peripheral blood mononuclear cell (PBMC) subset frequencies and transcriptomics(38). Here we added measurements of T cell activation and polarization and subsequent analysis of the same donors

at multiple time points (**Figure 1B, Table S2**). The increased plasma levels of IgGs specifically targeting the TdaP vaccine antigens PT, PRN, FHA, FIM2/3, TT, and DT on day 7 and 14 post-booster vaccination verified an induction of a humoral response and confirmed successful booster immunization (**Figure S1A**).

Whole-cell pertussis vaccine priming increases Th1 polarization despite acellular booster vaccination

Previous studies have shown that priming with the wP vaccine in infancy is associated with a life-long increase in Th1 polarization of the vaccine response compared to aP-primed individuals that show an increased Th2 polarization(15-19). We evaluated the Th1/Th2 polarization ratio in our cohort using a FluoroSpot assay(16) quantifying cytokine-secreting cells responding to aP vaccine antigens(15) stimulation following a 14-day expansion period. We selected IFN-γ and IL-5 as representative cytokines for Th1 and Th2 responses respectively(16). The Th1/Th2 (IFN-γ/IL-5) polarization ratio, further referred to as Th1 polarization, was significantly increased in wP compared to aP-primed participants before and 28 days after TdaP booster vaccination (**Figure 1C**) and these differences were independent of age after booster vaccination (**Figure S1B**). To identify vaccine-responsive $CD4^+$ T cells, the co-expression of the T cell activation surface markers interleukin 2 receptor alpha (CD25) and TNF Receptor Superfamily Member 4 (OX40) was determined of $CD4^+$ T cells before and 28 days post-booster vaccination by applying an activation induced marker (AIM) assay(39). The percentage of pertussis and tetanus antigen-specific activated $CD4^+$ T cells was significantly increased post- vs pre-booster vaccination in wP-primed participants, while aP-primed individuals' tetanus antigen-specific $CD4^+$ T cells, but not pertussis antigen-specific $CD4^+$ T cells, were significantly boosted (**Figure 1D**). Interestingly, the $CD4^+$ T cell response against pertussis antigens of wP-primed participants showed a significantly greater boost compared to aP-primed participants, while no differences were observed regarding the response against tetanus antigens (**Figure 1E**). To conclude, the previously described cell-mediated immunity against aP antigens and the Th1 polarization shift(15-19) in wP-primed individuals were confirmed in the wP-primed participants of this cohort.

Interferon signaling day 1 post-booster vaccination positively correlates with Th1 polarization

To create a comprehensive picture of the immune response induced by TdaP booster vaccination, RNAseq was performed on PBMCs before and 1, 3, 7, and 14 days after booster vaccination. RNAseq analysis identified a combined set of 1938 differentially expressed genes (DEGs) that showed significantly different expression at one or more of the post-booster time points compared to baseline (**Figure 2A**, FDR<0.05). The highest number of DEGs was recorded for day 1, with 579 downregulated and 922 upregulated genes that accounted together for 75.5% of the DEGs. In contrast, only 0.3% of DEGs were exclusive to day 3, 22.7% for day 7, and 1.6% for day 14. The most significant DEGs on day 1 included the increased expression of interferon-associated transcripts including *FCGR1A, STAT1, IRF1, GBP1,* and *CXCL10.* Day 7 DEGs included the increased expression of transcripts encoding immunoglobulin segments, such as *IGHG1, IGHV6-1*, *IGHGP*, *IGHG4*, and *IGKC,* confirming effective humoral booster vaccination, now on the RNA level.

Next, Spearman correlation analysis was performed to identify which of the DEGs were associated with Th1 polarization on day 28. This identified, for example, that transcriptional changes on day 1 vs pre-booster (day 1/pre-b) in Ganglioside GM2 Activator (*GM2A*), encoding a small glycolipid transport protein, were highly correlated with Th1 polarization on day 28 (**Figure 2B, left panel**). By performing these analyses systematically, we found that most transcriptional changes that showed a significant correlation ($P<0.05$) with Th1 polarization on day 28 originated from day 1/pre-b DEG, both absolutely and relatively to its number of DEG (**Figure 2B, right panel**). Almost all (294/300) day 1/pre-b transcriptional perturbations that correlated with Th1 polarization enclosed a positive association.

The 294 DEGs identified on day 1 with a positive correlation with Th1 polarization were examined for shared properties that explain their coordinated upregulation. Pathway enrichment analysis identified different immunological pathways including innate immune response (GO:0045087), cell activation (GO:0001775, which includes T cell activation (GO:0042110) as a pathway member), immune effector process (adaptive immune response, GO:0002252) and response to type II interferon (GO:0034341, **Figure 2C)**. Separately, DNA motif enrichment analysis using the 294 DEGs identified interferon-stimulated response element (ISRE) and interferon regulatory factors (IRFs) as the most enriched motifs (**Figure 2D**). This is corroborated by the gene expression of multiple interferon-related transcription factors including *STAT2, IRF1, IRF8, and IRF9*, all of which peak at day 1 post-booster and are correlated with increased Th1 polarization (**Figure 2E-F, Figure S2**). Other interferon-related Th1 polarization correlates are *FCGR1A, FI35, IFIT3, IRF8, IL27, OAS2, OASL, GBP4, and MX2* (**Figure 2F**) and were induced on day 1 post-booster (**Figure 2A).** Taken together, Th1 polarization of BP-specific $CD4^+$ T cells on day 28 correlated strongly with the level of interferon signaling detected in the transcriptional profile of PBMCs on day 1 post-booster vaccination.

Plasma IFN-γ concentrations increase on day 1 post-booster vaccination and correlate with the Th1 polarization

Next, we examined which vaccine-induced cytokines correlated with Th1 polarization on day 28 post-booster. The concentrations of 45 different cytokines were measured before and 1, 3, 7, and 14 days after booster vaccination to characterize the immune response induced by TdaP booster vaccination at the protein level (**Figure 3A)**. Of all cytokines and time points, the concentration of IFN-γ at day 1 post-boost showed the highest and most significant induction after booster vaccination (**Figure 3A-B**). To correct for baseline differences in IFN-γ plasma levels, fold changes of post/pre-booster were calculated per cytokine and post-booster time point and were used for correlation analysis with the Th1 polarization data. IFN-γ was the only cytokine that showed a significant correlation on day 1/pre-booster with the Th1 polarization ratio (**Figure 3C, Table S3**). While plasma IFN-γ levels peaked at day 1 post-booster, *IFNG* gene expression was not significantly increased on day 1 post-booster or any other time point measured (**Figure 3D**). The presence of high levels of plasma IFN-γ on day 1 post-booster together with the lack of a transcriptional *IFNG* peak in PBMCs suggests that *IFNG* transcription occurred within hours post-booster vaccination and/or that IFN-γ is produced by tissue-resident cells present at the injection site or its draining lymph nodes. To conclude, plasma IFN-γ

concentrations peak on day 1 post-booster vaccination and are positively associated with increased Th1 polarization on day 28.

IFN-γ initiated cytokine production on days 1 and 3 positively associated with Th1 polarization

As IFN-γ expression and signaling on day 1 post-vaccination is the strongest correlate of Th1 polarization on day 28, we wanted to examine the behavior of other players in the IFN-γ pathway. IFN-γ is known to bind to the IFN-γ receptor which consists of the two subunits IFNGR1 and IFNGR2(40). When IFN-γ activates its receptor, downstream signaling ensures the phosphorylation of STAT1, which then forms a homodimer. These complexes translocate to the nucleus where they initiate transcription by binding to genes containing GAS elements in their promotors. *CXCL9*, *CXCL10*, and *CXCL11* are examples of transcripts that will be transcribed after IFN-γ stimulation(41). These chemokines promote the migration of CXCR3-expressing cells, such as activated T cells and natural killer cells.

Plasma levels of CXCL9, CXCL10, and CXCL11 significantly increased on day 1 and day 3 post-booster compared to pre-booster (**Figure 3E**). Additionally, participants showing induction of plasma IFN-γ also showed an induction of plasma in CXCL9, CXCL10, and CXCL11, at any time point measured (**Figure 3F**). The day 3/pre-b plasma concentration of CXCL9 and CXCL11 positively correlated with the Th1 polarization on both day 1/pre-b and day 28/pre-b (**Figure 3G-H**). To conclude, we found evidence of a positive correlation between both systemic IFN-γ perturbations and interferon signaling with Th1 polarization at the protein level, mirroring the patterns observed in RNA transcripts.

TdaP booster-induced changes in plasma IFN-γ and CXCL9-11 correlate with the magnitude of transcriptional IFN response

Since both changes in plasma IFN-γ and IFN-induced gene expression in PBMCs correlate with the Th1 polarization, we next investigated the relationship between the production of plasma IFN-γ and IFN-induced gene expression in PBMCs on day 1 post-booster vaccination. The production of plasma IFN-γ, CXCL9, CXCL10, and CXCL11 all significantly correlated with the gene expression magnitude of more than 20 IFN-associated genes in PBMCs (**Figure 4A-B**). The 5 strongest correlations all involved plasma IFN-γ and significantly correlated with transcriptional changes in *STAT1, FCGR1A, GBP1, GBP2, and IRF1*. Moreover, the IFN-induced plasma cytokines CXCL9, CXCL10, and CXCL11 also significantly correlated with these transcriptional changes. This confirms that individuals with increased plasma IFN-γ levels post-TdaP vaccination, also showed an increase in IFN-induced gene expression in PBMCs. These findings suggest that the vaccine-induced production of IFN-γ induced a systemic immune response in which IFN-associated gene expression was likely also initiated in non-T cell subsets. This subsequent systemic effect–which also correlated with the Th1 polarization–may contribute to maintaining the Th polarization differences observed in aP compared to wP individuals.

Discussion

It is now well established that individuals primed during infancy with the wP vaccine maintain an increased Th1 polarization in their memory T cell response compared to aP primed individuals (15-19). It has however remained a puzzle how this polarization is maintained over decades in wP primed individuals despite repeated TdaP booster vaccinations. To address this question, we performed a longitudinal multi-omics analysis of the immune state pre- and post-Tdap booster vaccination to identify the cascade of events that leads to a Th1 polarized memory T cell response, which is associated with durable protection. In our hypothesis-generating study design, we comprehensively mapped the immune state by measuring many blood parameters, identified which ones were perturbed by vaccination, and then queried which ones were positively correlated with the Th1 response 28 days post-vaccination.

We found that Th1 polarization correlated positively with a vaccine-induced interferon response in PBMCs on day 1-3 post-booster on transcriptional and protein levels. This suggests that early IFN-γ secretion maintains the Th1 polarized response in DTwP-primed individuals despite multiple TdaP boosters, through a positive feedback loop (**Graphical abstract**). Therefore, stimulating IFN-γ signaling during vaccination might boost Th1 responses against BP which could improve protection against infection and increase vaccine durability.

A caveat to our finding is that we cannot rule out that type I interferons (IFN-α and IFN-β) rather than IFN-γ are the initial cause of the observed IFN signature on day 1 post-booster. In contrast to IFN-γ, IFN-α and IFN-β can also induce the transcription of genes that have ISRE but lack GAS elements in their promoter. However, since IFN-α, IFN-β, and IFN-γ can all induce transcription of genes containing GAS elements, the possibility cannot be ruled out that both type I and II IFN contribute to the observed booster-induced IFN response that correlates with Th1 polarization. Although a correlation was also found between IFN-γ and Th1 polarization, this IFN-γ could be type I IFN induced as it has been shown that IFN-β stimulates IFN-γ production in human naive $CD4^+$ T cells(37). Notably, we did not detect type I interferons at the protein and RNA level in the blood, but that does not rule out their presence in other tissues.

Another limitation of this study is that its design will miss the unmeasured, such as changes in phosphorylation and epigenetics, but also changes in time points and other tissues that were not included. Although our study lacks nasal data, Wilk *et al.* have described that previous BP infection and wP vaccination, but not aP immunization, lead to the formation of $CD69^+CD4^+$ tissue-resident memory T cells which protect the nose and lungs against BP colonization in C57BL/6 mice(7). This is in line with the findings based on blood describing that the immune response induced by the wP vaccine resembles that induced by natural infection, while the aP-induced immune response is divergent(7, 8). This together suggests that the systemic responses induced by infection and wP vaccination induce overlapping pathways leading to Th1 polarization and, therefore, protection against infection.

Can Th2 cells be repolarized to Th1 cells to increase the protection against BP infection and duration of immunity? Naive $CD4^+$ T cells exhibit significant plasticity in their differentiation into

various Th subsets. However, the repolarization capacity of Th1 and Th2 cells seems to disappear once T cells are stimulated multiple times and terminally differentiated(42). This stability is mediated by epigenetic modifications and the expression of lineage-specific transcription factors(43). Additionally, IFN-γ inhibits Th2 polarization and IL-5 inhibits Th1 polarization. Memory Th2 cells retain both antigen specificity and response type, making early vaccination strategy changes more effective in increasing protection against BP infections. However, for individuals already primed with aP vaccines, activating the IFN pathway during booster vaccinations presents a viable alternative to promote Th1 polarization in newly recruited naive T cells, potentially improving the efficacy of current aP vaccines.

How could the IFN pathway be stimulated during vaccination? The first and obvious answer is the use of adjuvants - indispensable vaccine components that stimulate the initiation of an immune response by working as an antigen-delivery system or stimulating Toll-like receptors (TLRs) and other pattern recognition receptors (PRRs)(44, 45). Although the conventional DTaP and DTwP vaccines both contain aluminum salts as adjuvants(46), the exact formulation and type of aluminum salt may vary and be involved in causing the Th1 polarization differences. Aluminum adjuvants are known to induce a Th2 response. FDA-approved adjuvants that induce a Th1 response, such as monophosphoryl lipid A (MPLA) containing adjuvants(47) and the synthetic single-stranded DNA molecule CpG 1018(48) are also available. Changing the pertussis vaccination strategy by switching to or adding an adjuvant that coordinates the immune response to the Th1 phenotype might result in a vaccine that protects longer and better against infection. Interestingly, multiple studies have demonstrated that adding CpG 1018 to TdaP increased protection in mice, with a shift toward Th1, compared to alum-only adjuvanted Tdap(49, 50).

Our studies suggest that changing the current BP vaccination strategy by one that induces IFN-γ production might prevent the lack of robust Th1 responses observed in aP-primed individuals. Further research is needed to verify if targeting IFN-γ during BP vaccination enhances both the longevity of the immune response and protection against infection. Additionally, the specific cell populations responsible for IFN-γ production and their tissue location should be identified. This can first be investigated in the multiple established mouse and non-human primate models, and ultimately in controlled human infection models of BP (51-53).

Materials and methods

Study design and human participants

Healthy adults who were primed with either the aP (n=32) or wP (n=30) vaccine during childhood were recruited (Figure 1A). All participants confirmed that they had not received TdaP booster vaccination in the last 4 years and provided written informed consent before donation. TdaP booster vaccination was administered on day 0 and contains tetanus toxoid (TT), diphtheria toxoid (DT), and aP containing inactivated pertussis toxin (PT) and cell surface proteins of BP including filamentous hemagglutinin (FHA), fimbriae 2/3 (Fim2/3), and pertactin (PRN). Longitudinal blood samples were collected pre- (days -31, -14, 0) and post-booster

vaccination (days 1, 3, 7, 14, 28). Figure 2A shows the experiments that were performed per time point to map the immune response before and after booster vaccination. Characteristics of the study population are shown in Table S1-S2. Plasma antigen-specific IgG levels including IgG isotypes (IgG1-4), plasma concentrations of 45 different cytokines, and peripheral blood mononuclear cell (PBMC) subset frequencies and transcriptomics experiments were performed previously(38). Here we added measurements of T cell activation and polarization of the same donors at different time points (Figure 1B, Table S2).

Whole blood processing

Whole blood samples (with heparin) were centrifuged at 1850 rpm for 15 min with breaks off. Subsequently, the upper fraction (plasma) was collected and stored at -80°C. Peripheral blood mononuclear cells (PBMC) were isolated by density gradient centrifugation using Ficoll-Paque PLUS (Amersham Biosciences). 35 mL of RPMI 1640 medium (RPMI, Omega Scientific) diluted blood was slowly layered on top of 15 mL Ficoll-Paque PLUS. Sampled were centrifuged at 1850 rpm for 25 min with breaks off. Then, PBMC layers were aspirated and 2 PBMC layers per donor were combined in a new tube together with RPMI. Samples were centrifuged at 1850 rpm for 10 min with a low break. Cell pellets of the same donors were combined and washed with RPMI and centrifuged at 1850 rpm for 10 min with breaks off. Finally, PBMC were counted using trypan blue and a hemocytometer and, after another spin, resuspended in Fetal Bovine Serum (FBS, Gemini) containing 10% DMSO (MilliporeSigma) and stored in a Mr. Frosty cell freezing container overnight at -80°C. The next day, samples were stored in liquid nitrogen until further use.

AIM assay

Cryopreserved PBMCs were thawed at 37°C for 1 min and added to 10 mL cell culture medium (RPMI 1640 (Corning, 10-041-CM) supplemented with 5% Human Serum AB (GeminiBio, 110-512), 1% Penicillin:Streptomycin solution (GeminiBio, 400-109), and 1% GlutaMAX (Gibco, 35050061)) with 20 uL of Benzonase nuclease (MilliporeSigma). PBMCs were centrifuged at 1400 rpm for 5 min at RT and resuspended in cell culture medium to determine cell concentration and viability using 0.02% Trypan Blue (ThermoFisher) and a hemocytometer. One million PBMCs were seeded in 100uL cell culture medium per well into a 96-well plate (GenClone, 25-221) and were stimulated with 1 of the following 4 stimuli: Tetanus megapool(54) (1 µg/mL), aP megapool(15) (1 µg/mL), 0.3% DMSO (negative control, MilliporeSigma, D2650), and PHA-L (1 µg/mL, positive control, MilliporeSigma, 431784). Stimulated cells were incubated for 18-24 hours at 37°C and 5% CO_2 and subsequently spun at 1400 rpm for 2 min at RT. Cells were washed twice with PBS (Gibco) and resuspended in 10% FBS in PBS. Then, cells were incubated for 10 min at 4°C. Cells were stained with a 100 uL antibody cocktail (antibody details are shown in Table S4) for 30 minutes at 4°C in the dark. Stained cells were centrifuged at 1400 rpm for 2 min at 4°C and washed twice with PBS. Cells were resuspended in MACS buffer (2 mM EDTA (Omega) and 0.5% BSA (MilliporeSigma) in PBS at pH 7.0) and transferred to cluster tubes (Corning Life Sciences Plastic, 4401). For compensation, beads (Thermo Fisher, 01-2222-42) were washed twice with PBS and centrifuged at 1400 rpm for 2 min at RT. Beads were distributed in wells and single-stained with 2 uL antibody. Data was acquired using LSR II Flow Cytometer (BD) and analyzed using FlowJo software (v10.10.0). The AIM gating strategy

is depicted in Figure S3. DMSO values were subtracted from aP megapool measurements. The median of all DMSO (negative control) measurements (0.012%) was set as the lower detection threshold (LOD) and was added to all measurements before fold change calculations to prevent inflated fold change estimates caused by measurements close to or below the lower detection threshold. In plots where percentages are shown, values below LOD were set to LOD after DMSO subtraction.

Fluorospot

Two million PBMC were seeded in 500 µL cell culture medium (composition described above). PBMC were incubated with 2 µg/mL aP megapool(15) for 14 days at 37°C and 5% CO_2. Cells were fed on day 4 with 1 mL of cell culture medium containing 10U/mL IL-2 (Prospec CYT-209B) and 1 mL medium was replaced on days 7 and 11. Fluorospot PVDF plates (Mabtech, 3654-FL-10) were washed with 70% methanol (MilliporeSigma, 154903) and subsequently 3x with sterile dH_2O. Next, the plates were coated with a capture antibody cocktail containing 10 µg/mL mouse anti-human of each IFN-γ (Mabtech, clone: 1-D1K), IL-5 (Mabtech, clone: TRFK5), and IL-17 (Mabtech, clone: MT44.6) in PBS (Gibco) and incubated overnight at 4°C. The next day, the plates were washed 3x with PBS. Then, plates were blocked by incubating them with cell culture medium for 1 hour at 37°C. After 1 hour, the medium was replaced by a medium containing either 2 µg/mL aP megapool, 0.2% DMSO (negative control, MilliporeSigma, D2650), or 20 µg/mL PHA-L (positive control, MilliporeSigma, 431784). Meanwhile, after 14 days of cell culture, cells were harvested, washed, and counted using a hemocytometer. 2 million cells were added per well in a 1:1 ratio and cultured for 24 hours at 37°C and 5% CO_2. After 24 hours, the plates were washed 5x with 0.05% Tween20 (MilliporeSigma, PPB005) in PBS. Plates were incubated with the following Mabtech detection antibodies: anti-IFN-γ 7-B6-1-BAM (1:200), anti-IL-5 5A10-WASP (1:200), and 2 µg/mL anti-IL-17 MT504 biotinylated in 0.1% bovine serum albumin (BSA, MilliporeSigma, A3294) in PBS for 2 hours at room temperature (RT). After 2 hours, plates were washed 5x with 0.05% Tween in PBS. Next, plates were incubated with the following Mabtech fluorophore-conjugated detection antibodies: anti-BAM-490, anti-WASP-640, and SA-550 1:200 in 0.1% BSA in PBS for 1 hour at RT, covered from light. After incubation, plates were washed 5x with 0.05% Tween20 in PBS. Then, fluorescence enhancer (Mabtech, 3641-F10) was added and removed after 15 minutes of incubation at RT. Plates were air-dried and measured using a (Mabtech IRIS Fluorospot/ELISpot Reader). A cytokine response was considered positive when the following three criteria were met: 1) eliciting at least 20 spot-forming cells (SFC) per million PBMC, 2) $P \leq 0.05$ by Student's t-test or by the Poisson distribution test, and 3) stimulation index (SI) ≥ 2.

Plasma cytokine concentrations

Plasma samples were randomly distributed on 96 well plates for the absolute quantification of 45 different cytokines (Olink Target 48 Cytokine panel) by Hamilton Health Science (Canada). The Proximity Extension Assay (PEA) technology(55) was used for protein quantification. Briefly, the plasma was incubated with oligonucleotides labeled antibodies targeting the proteins of interest. The oligonucleotides of matched oligonucleotides-antibodies-antigen will bind to each other, enabling amplification and thereby quantification by qPCR. Ct values from the qPCR were used to calculate Normalized Protein eXpression (NPX), a relative quantification unit to

report protein expression levels in plasma samples. A standard curve model was established per protein and used to normalize between plates and batches, but also to translate the measured sample NPX values to protein concentrations in pg/mL. More details are described in the Target 48 User Manual (Olink®, v13). Before fold change calculations, the 5% quantile was calculated and added per cytokine to prevent inflated fold change estimates caused by measurements close to or below the lower detection threshold. For cytokines of which the 5% quantile was equal to zero, +1 was applied before fold change calculations.

Plasma antibody measurements

Pertussis antigen-specific antibody responses were quantified in human plasma by performing an indirect serological assay with xMAP Microspheres (details described in xMAP Cookbook, Luminex 5th edition). Pertussis, Tetanus, and Diphtheria antigens (PT, PRN, Fim2/3, TT, DT (all from List Biological Laboratories), and FHA (MilliporeSigma)) and as a negative control Ovalbumin (OVA, MilliporeSigma) were coupled to uniquely coded beads (xMAP MagPlex Microspheres, Luminex Corporation). PT was inactivated by incubation with 1% formaldehyde (PFA) at 4°C for 10 min. 1% PFA PT and TT were then purified using Zeba spin desalting columns (ThermoFisher). The antigens were coupled with each unique conjugated microsphere at a concentration of 12.5×10^6 beads/mL using the xMAP Antibody Coupling Kit (Luminex Corporation). Plasma was mixed with a mixture of each conjugated microsphere and the WHO International Standard Human Pertussis antiserum was used as a reference standard (NIBSC, 06/140). Subsequently, the mixtures were washed with 0.05% TWEEN20 in PBS (MilliporeSigma) to exclude non-specific antibodies and targeted antibody responses were detected via anti-human total IgG-PE, IgG1-PE, IgG2-PE, IgG3-PE, and IgG4-PE (all from SouthernBiotech). Antibody details are shown in **Table S4**. Samples were subsequently measured on a MAGPIX® instrument (Luminex Corporation) and the $\log_{10}$ of the median fluorescent intensity (MFI) values were collected. Measurements were corrected to 0 when the average + 3-fold standard deviation of the background samples (sample dilution buffer) was higher than the measurement.

RNA sequencing

Per sample, 2 million PBMC were lysed using QIAzol Lysis Reagent (Qiagen). Samples were stored at -80°C until RNA extraction. RNA was extracted using the miRNeasy Mini Kit (Qiagen) including DNase treatment according to the manufacturer's instructions. The Smart-seq2 protocol was used to perform full-length bulkRNAseq. Briefly, RNA was captured using oligo-poly(dT)-30 primers and reverse transcription was performed using 50-template switching oligos (LNA technologies, Exicon). cDNA was pre-amplified using PCR and purified twice by magnetic beads (volume ratio 0.6x and 0.8x Ampure-XP magnetic beads, Beckman Coulter). cDNA was measured using capillary electrophoresis (Fragment analyzer, Advance analytical) and 0.5 ng of cDNA was used to generate indexed Illumina libraries (Nextera XT library preparation kit, Illumina). Each library's fragment size was measured by capillary electrophoresis (Fragment analyzer, Advance analytical) and was quantified (Picogreen, Thermofisher). Libraries were pooled at equal molar concentration and sequenced paired-end on a NovaSeq6000 (Illumina) sequencing system to a minimum depth of 15 million reads with each a length of 100 base pairs (S4 flowcell 200 cycle v1.0, Xp workflow; Illumina).

Bioinformatics RNA sequencing

Raw sequencing reads were aligned to the hg19 genome reference using our in-house pipeline (https://github.com/ndu-UCSD/LJI_RNA_SEQ_PIPELINE_V2). Briefly, FASTQ files were merged and filtered using fastp (v0.20.1), reads were aligned using STAR (v2.7.3a) and further processed using SAMtools (v0.1.19–44428cd), bamCoverage (v3.3.1), and Qualimap (v.2.2.2-dev). From this pipeline, raw counts and transcripts per million (TPM) reads were provided as output. Lowly expressed genes were removed for subsequent analysis (<=10 raw read counts). Differential expression was assessed using the DESeq2 Bioconductor package (v1.36.0)(56) in an R v4.2.1 environment with gene expression called differential with an FDR<0.05. Before fold change calculations, the 5% TPM quantile was calculated per gene and batch year (2021 and 2022) to prevent inflated fold change estimates caused by measurements close to zero. For genes of which the 5% quantile was equal to zero, TPM+0.1 was applied before fold change calculations. Spearman correlation analysis was performed using the correlation package (v0.8.4)(57). Pathway enrichment analysis was performed using Metascape and the Gene Ontology (GO) gene sets(58). Motif enrichment analysis was performed using HOMER findMotifs.pl (v4.11.1) with all genes with at least 10 raw counts as background(59).

Data availability

Experimental data is publicly available on the CMI-PB website (https://www.cmi-pb.org/data).

Acknowledgments

This work was supported by the National Institute of Allergy and Infectious Diseases (NIAID) of the National Institutes of Health (NIH) under award no. U01AI150753, U01AI141995 and U19AI142742. The authors are grateful to all donors who participated in the study and the following La Jolla Institute for Immunology core facilities for their contribution: Clinical Studies, Flow Cytometry, Bioinformatics, and Next Generation Sequencing.

Author contributions

Study design: B.P., L.W.; Data collection: F.S.C., L.W., M.A., J.L.; Data analysis and graphical representation: L.W.; Manuscript writing and feedback: L.W., B.P., J.L., R.S.A., S.O., M.K.; Study initiation and supervision: B.P.

Competing interests

The authors declare no competing interests.

References

1. Noble BA, Jiudice SS, Jones JD, Timbrook TT. Reemergence of Bordetella parapertussis, United States, 2019-2023. Emerg Infect Dis. 2024;30(5):1058-60.
2. Smout E, Mellon D, Rae M. Whooping cough rises sharply in UK and Europe. BMJ. 2024;385:q736.
3. Decker MD, Edwards KM. Pertussis (Whooping Cough). J Infect Dis. 2021;224(12 Suppl 2):S310-S20.
4. (CDC) CfDCaP. Whooping Cough (Pertussis) Vaccination 2022 [updated September 6, 2022. Available from: https://www.cdc.gov/vaccines/vpd/pertussis/index.html.
5. Gambhir M, Clark TA, Cauchemez S, Tartof SY, Swerdlow DL, Ferguson NM. A change in vaccine efficacy and duration of protection explains recent rises in pertussis incidence in the United States. PLoS Comput Biol. 2015;11(4):e1004138.
6. Witt MA, Arias L, Katz PH, Truong ET, Witt DJ. Reduced risk of pertussis among persons ever vaccinated with whole cell pertussis vaccine compared to recipients of acellular pertussis vaccines in a large US cohort. Clin Infect Dis. 2013;56(9):1248-54.
7. Wilk MM, Borkner L, Misiak A, Curham L, Allen AC, Mills KHG. Immunization with whole cell but not acellular pertussis vaccines primes CD4 T(RM) cells that sustain protective immunity against nasal colonization with Bordetella pertussis. Emerg Microbes Infect. 2019;8(1):169-85.
8. Warfel JM, Zimmerman LI, Merkel TJ. Acellular pertussis vaccines protect against disease but fail to prevent infection and transmission in a nonhuman primate model. Proc Natl Acad Sci U S A. 2014;111(2):787-92.
9. Kuehn BM. Resurgence of Pertussis Linked With Switch to Acellular Vaccine. JAMA. 2021;326(4):300.
10. Klein NP, Bartlett J, Rowhani-Rahbar A, Fireman B, Baxter R. Waning protection after fifth dose of acellular pertussis vaccine in children. N Engl J Med. 2012;367(11):1012-9.
11. Klein NP, Bartlett J, Fireman B, Baxter R. Waning Tdap Effectiveness in Adolescents. Pediatrics. 2016;137(3):e20153326.
12. Esposito S, Stefanelli P, Fry NK, Fedele G, He Q, Paterson P, et al. Pertussis Prevention: Reasons for Resurgence, and Differences in the Current Acellular Pertussis Vaccines. Front Immunol. 2019;10:1344.
13. Burdin N, Handy LK, Plotkin SA. What Is Wrong with Pertussis Vaccine Immunity? The Problem of Waning Effectiveness of Pertussis Vaccines. Cold Spring Harb Perspect Biol. 2017;9(12).
14. Fedele G, Cassone A, Ausiello CM. T-cell immune responses to Bordetella pertussis infection and vaccination. Pathog Dis. 2015;73(7).
15. da Silva Antunes R, Babor M, Carpenter C, Khalil N, Cortese M, Mentzer AJ, et al. Th1/Th17 polarization persists following whole-cell pertussis vaccination despite repeated acellular boosters. J Clin Invest. 2018;128(9):3853-65.
16. Bancroft T, Dillon MB, da Silva Antunes R, Paul S, Peters B, Crotty S, et al. Th1 versus Th2 T cell polarization by whole-cell and acellular childhood pertussis vaccines persists upon re-immunization in adolescence and adulthood. Cell Immunol. 2016;304-305:35-43.

17. van der Lee S, Hendrikx LH, Sanders EAM, Berbers GAM, Buisman AM. Whole-Cell or Acellular Pertussis Primary Immunizations in Infancy Determines Adolescent Cellular Immune Profiles. Front Immunol. 2018;9:51.
18. da Silva Antunes R, Quiambao LG, Sutherland A, Soldevila F, Dhanda SK, Armstrong SK, et al. Development and Validation of a Bordetella pertussis Whole-Genome Screening Strategy. J Immunol Res. 2020;2020:8202067.
19. da Silva Antunes R, Garrigan E, Quiambao LG, Dhanda SK, Marrama D, Westernberg L, et al. T cell reactivity to Bordetella pertussis is highly diverse regardless of childhood vaccination. Cell Host & Microbe. 2023;31(8):1404-16.e4.
20. Schure RM, Hendrikx LH, de Rond LG, Ozturk K, Sanders EA, Berbers GA, et al. T-cell responses before and after the fifth consecutive acellular pertussis vaccination in 4-year-old Dutch children. Clin Vaccine Immunol. 2012;19(11):1879-86.
21. Pulendran B, Artis D. New Paradigms in Type 2 Immunity. Science. 2012;337(6093):431-5.
22. Swain SL. T-Cell Subsets: Who does the polarizing? Current Biology. 1995;5(8):849-51.
23. Ross PJ, Sutton CE, Higgins S, Allen AC, Walsh K, Misiak A, et al. Relative contribution of Th1 and Th17 cells in adaptive immunity to Bordetella pertussis: towards the rational design of an improved acellular pertussis vaccine. PLoS Pathog. 2013;9(4):e1003264.
24. Ryan M, Murphy G, Gothefors L, Nilsson L, Storsaeter J, Mills KH. Bordetella pertussis respiratory infection in children is associated with preferential activation of type 1 T helper cells. J Infect Dis. 1997;175(5):1246-50.
25. Manetti R, Parronchi P, Giudizi MG, Piccinni MP, Maggi E, Trinchieri G, et al. Natural killer cell stimulatory factor (interleukin 12 [IL-12]) induces T helper type 1 (Th1)-specific immune responses and inhibits the development of IL-4-producing Th cells. J Exp Med. 1993;177(4):1199-204.
26. Seder RA, Gazzinelli R, Sher A, Paul WE. Interleukin 12 acts directly on CD4+ T cells to enhance priming for interferon gamma production and diminishes interleukin 4 inhibition of such priming. Proc Natl Acad Sci U S A. 1993;90(21):10188-92.
27. Hsieh CS, Macatonia SE, Tripp CS, Wolf SF, O'Garra A, Murphy KM. Development of TH1 CD4+ T cells through IL-12 produced by Listeria-induced macrophages. Science. 1993;260(5107):547-9.
28. Wu CY, Demeure C, Kiniwa M, Gately M, Delespesse G. IL-12 induces the production of IFN-gamma by neonatal human CD4 T cells. J Immunol. 1993;151(4):1938-49.
29. Okamura H, Kashiwamura S, Tsutsui H, Yoshimoto T, Nakanishi K. Regulation of interferon-gamma production by IL-12 and IL-18. Curr Opin Immunol. 1998;10(3):259-64.
30. Kopf M, Le Gros G, Bachmann M, Lamers MC, Bluethmann H, Kohler G. Disruption of the murine IL-4 gene blocks Th2 cytokine responses. Nature. 1993;362(6417):245-8.
31. Kastenmuller W, Torabi-Parizi P, Subramanian N, Lammermann T, Germain RN. A spatially-organized multicellular innate immune response in lymph nodes limits systemic pathogen spread. Cell. 2012;150(6):1235-48.
32. Coccia M, Collignon C, Herve C, Chalon A, Welsby I, Detienne S, et al. Cellular and molecular synergy in AS01-adjuvanted vaccines results in an early IFNgamma response promoting vaccine immunogenicity. NPJ Vaccines. 2017;2:25.
33. Murphy KM, Weaver C, Berg LJ. Janeway's Immunobiology. 10 ed: W. W. Norton & Company; 2022.

34. Barbic J, Leef MF, Burns DL, Shahin RD. Role of gamma interferon in natural clearance of Bordetella pertussis infection. Infection and Immunity. 1997;65(12):4904-8.
35. Byrne P, Mcguirk P, Todryk S, Mills KHG. Depletion of NK cells results in disseminating lethal infection with Bordetella pertussis associated with a reduction of antigen‐specific Th1 and enhancement of Th2, but not Tr1 cells. European Journal of Immunology. 2004;34(9):2579-88.
36. Gillard J, Suffiotti M, Brazda P, Venkatasubramanian PB, Versteegen P, De Jonge MI, et al. Antiviral responses induced by Tdap-IPV vaccination are associated with persistent humoral immunity to Bordetella pertussis. Nature Communications. 2024;15(1).
37. da Silva Antunes R, Quiambao LG, Soldevila F, Sutherland A, Peters B, Sette A. Lack of evidence supporting a role of IFN-beta and TGF-beta in differential polarization of Bordetella pertussis specific-T cell responses. Cytokine. 2021;137:155313.
38. da Silva Antunes R, Soldevila F, Pomaznoy M, Babor M, Bennett J, Tian Y, et al. A system-view of Bordetella pertussis booster vaccine responses in adults primed with whole-cell versus acellular vaccine in infancy. JCI Insight. 2021;6(7).
39. Dan JM, Lindestam Arlehamn CS, Weiskopf D, da Silva Antunes R, Havenar-Daughton C, Reiss SM, et al. A Cytokine-Independent Approach To Identify Antigen-Specific Human Germinal Center T Follicular Helper Cells and Rare Antigen-Specific CD4+ T Cells in Blood. J Immunol. 2016;197(3):983-93.
40. Platanias LC. Mechanisms of type-I- and type-II-interferon-mediated signalling. Nat Rev Immunol. 2005;5(5):375-86.
41. Metzemaekers M, Vanheule V, Janssens R, Struyf S, Proost P. Overview of the Mechanisms that May Contribute to the Non-Redundant Activities of Interferon-Inducible CXC Chemokine Receptor 3 Ligands. Front Immunol. 2017;8:1970.
42. Murphy E, Shibuya K, Hosken N, Openshaw P, Maino V, Davis K, et al. Reversibility of T helper 1 and 2 populations is lost after long-term stimulation. J Exp Med. 1996;183(3):901-13.
43. Zhu J, Paul WE. Heterogeneity and plasticity of T helper cells. Cell Res. 2010;20(1):4-12.
44. Verma SK, Mahajan P, Singh NK, Gupta A, Aggarwal R, Rappuoli R, et al. New-age vaccine adjuvants, their development, and future perspective. Frontiers in Immunology. 2023;14.
45. Zhao T, Cai Y, Jiang Y, He X, Wei Y, Yu Y, et al. Vaccine adjuvants: mechanisms and platforms. Signal Transduction and Targeted Therapy. 2023;8(1).
46. (WHO) WHO. Prequalified Vaccines (DTP acellular and whole-cell) 2023 [Available from: https://extranet.who.int/prequal/vaccines/prequalified-vaccines.
47. Patil HP, Murugappan S, ter Veer W, Meijerhof T, de Haan A, Frijlink HW, et al. Evaluation of monophosphoryl lipid A as adjuvant for pulmonary delivered influenza vaccine. J Control Release. 2014;174:51-62.
48. Li Y, Chen X. CpG 1018 Is an Effective Adjuvant for Influenza Nucleoprotein. Vaccines (Basel). 2023;11(3).
49. Asokanathan C, Corbel M, Xing D. A CpG-containing oligodeoxynucleotide adjuvant for acellular pertussis vaccine improves the protective response against Bordetella pertussis. Hum Vaccin Immunother. 2013;9(2):325-31.

50. DeJong MA, Wolf MA, Bitzer GJ, Hall JM, Sen-Kilic E, Blake JM, et al. CpG 1018(R) adjuvant enhances Tdap immune responses against Bordetella pertussis in mice. Vaccine. 2022;40(35):5229-40.
51. de Graaf H, Ibrahim M, Hill AR, Gbesemete D, Vaughan AT, Gorringe A, et al. Controlled Human Infection With Bordetella pertussis Induces Asymptomatic, Immunizing Colonization. Clin Infect Dis. 2020;71(2):403-11.
52. (CCfV) CCfV. Establishing a Controlled Human Infection Model of Bordetella pertussis 2022 [Available from: https://www.challengeunit.ca/pertussis-chim.
53. de Graaf H, Gbesemete D, Gorringe AR, Diavatopoulos DA, Kester KE, Faust SN, et al. Investigating Bordetella pertussis colonisation and immunity: protocol for an inpatient controlled human infection model. BMJ Open. 2017;7(10):e018594.
54. da Silva Antunes R, Paul S, Sidney J, Weiskopf D, Dan JM, Phillips E, et al. Definition of Human Epitopes Recognized in Tetanus Toxoid and Development of an Assay Strategy to Detect Ex Vivo Tetanus CD4+ T Cell Responses. PLoS One. 2017;12(1):e0169086.
55. Assarsson E, Lundberg M, Holmquist G, Bjorkesten J, Thorsen SB, Ekman D, et al. Homogenous 96-plex PEA immunoassay exhibiting high sensitivity, specificity, and excellent scalability. PLoS One. 2014;9(4):e95192.
56. Love MI, Huber W, Anders S. Moderated estimation of fold change and dispersion for RNA-seq data with DESeq2. Genome Biol. 2014;15(12):550.
57. Makowski D, Ben-Shachar M, Patil I, Lüdecke D. Methods and Algorithms for Correlation Analysis in R. Journal of Open Source Software. 2020;5(51):2306.
58. Zhou Y, Zhou B, Pache L, Chang M, Khodabakhshi AH, Tanaseichuk O, et al. Metascape provides a biologist-oriented resource for the analysis of systems-level datasets. Nat Commun. 2019;10(1):1523.
59. Heinz S, Benner C, Spann N, Bertolino E, Lin YC, Laslo P, et al. Simple combinations of lineage-determining transcription factors prime cis-regulatory elements required for macrophage and B cell identities. Mol Cell. 2010;38(4):576-89.

Figure 1

A

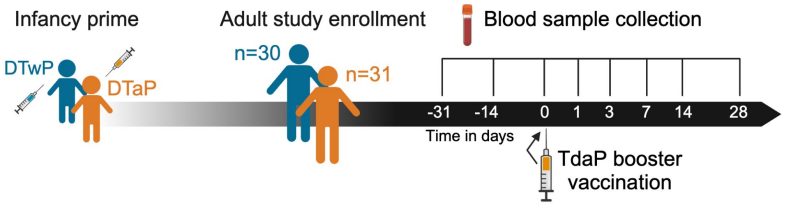

B

	Baseline			post-booster vaccination					days
	-31	-14	0	1	3	7	14	28	
Antibody MFI (plasma)	21	21	57	57	57	57	57	57	
T cell polarization (FluoroSpot)	15	14	50	0	0	0	0	50	
T cell activation (AIM)	17	20	57	0	0	0	0	57	
Gene expression (PBMC)	20	20	56	56	56	56	56	0	
Cytokine concentration (plasma)	17	20	60	59	61	60	61	0	

C

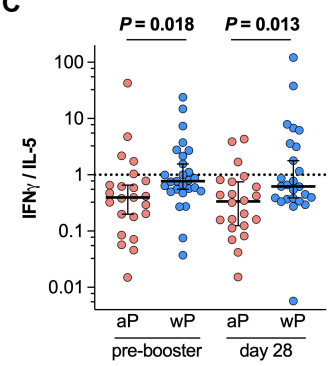

D

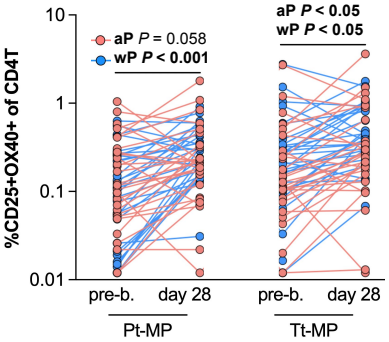

E

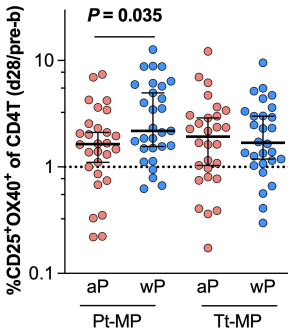

Figure 1. **Whole-cell pertussis vaccine priming increases Th1 polarization despite acellular booster vaccination. A)** Schematic illustration of TdaP booster vaccination study outline. Healthy adults were recruited who were primed with either the DTaP (n=31) or DTwP (n=30) vaccine during infancy. Blood was collected before and after TdaP booster vaccination. **B**) Table indicating sample quantity per experiment type and time point. Plasma was used for antibody and cytokine measurements and peripheral blood mononuclear cells (PBMCs) were used to determine gene expression, and T cell activation and polarization. **C**) IFN-γ and IL-5 producing cells (spot-forming cells, SFC) were measured by Fluorospot after cells were stimulated with aP vaccine antigens for 14 days and derived from blood sampled before and 28 days after TdaP booster vaccination (black lines represent the median ± interquartile range). The IFN-γ/IL-5 ratio was used as a measurement of Th1/Th2 polarization. (n= 22-23 aP, 25-27 wP, P-values were calculated by multiple Mann-Whitney tests). **D-E**) An activation induced marker (AIM) assay was performed in which PBMCs were stimulated with 1 µg/mL of either the pertussis or tetanus peptide megapools for 18-24 hours. $CD25^+$ and $OX40^+$ $CD4^+$ T cells were measured by flow cytometry and shown as percentage of total $CD4^+$ T cells (**D**) and as 28 days post/pre booster vaccination ratio (**E**) where black lines represent the median ± interquartile range). (n= 28 aP, 29 wP, P-values were calculated by **D**) multiple Wilcoxon matched-pairs test and **E**) multiple Mann-Whitney tests).

Figure 2

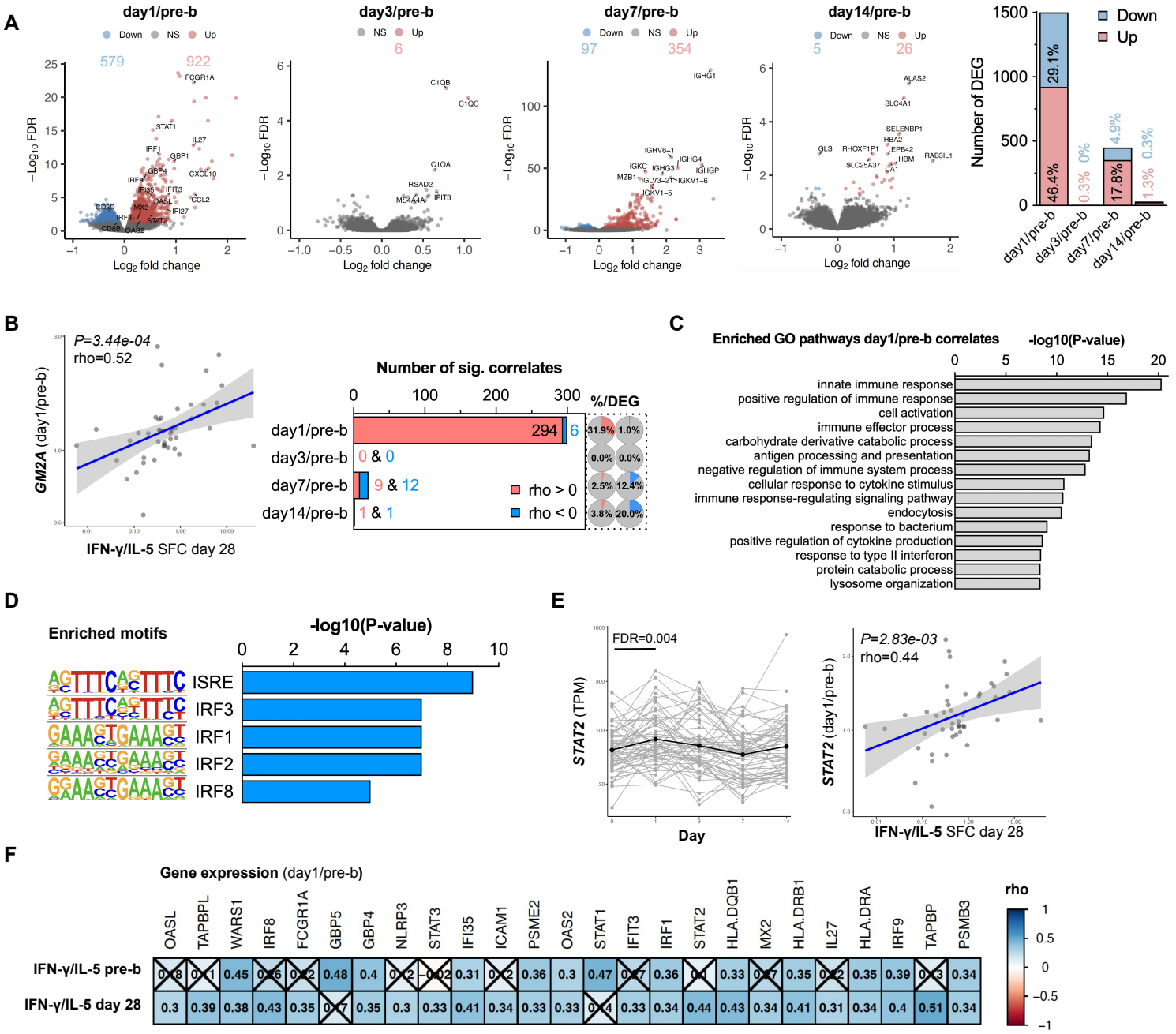

Figure 2. **Interferon signaling positively correlates with Th1 polarization.** **A)** Volcano plots showing the $\log_2$(fold-change) and $-\log_{10}$(FDR) of the differentially expressed genes (DEG) of day 1, 3, 7, 14 post/pre-booster vaccination with downregulated genes in blue and upregulated genes in red (FDR<0.05). The number and percentage of DEG of the total analysis are depicted in the bar chart. **B**) Spearman correlation analysis was performed using the DEG and T cell polarization data 28 days post booster (IFN-γ/IL-5 SFC). A dotplot of most significant correlate (*GM2A* day 1/pre-booster) is depicted and the number of significant correlates per time point comparison (*P*<0.05) and its percentage of the total number of DEG of that time point. **C)** The top 15 pathways identified by Gene Ontology (GO) pathway enrichment analysis using the 291 DEG (day 1/pre-booster) that also showed a positive correlation with the T cell polarization on day 28. **D**) The top 5 known motifs identified by HOMER motif enrichment analysis using the 291 DEG (day 1/pre-booster) that also showed a positive correlation with the T cell polarization on day 28. **E**) *STAT2* gene expression (TPM) over time with the black line indicating the mean expression (left) and Spearman correlation (right) between *STAT2* (day 1/pre-booster) and T cell polarization data 28 days post booster (IFN-γ/IL-5 SFC). **F**) Heatmap depicting Spearman correlation rho's of selected transcriptional changes (day1/pre-booster) vs T cell polarization data pre- and post-booster. Insignificant correlates are crossed (*P*>0.05). RNA n=56, correlation analysis n=44.

Figure 3

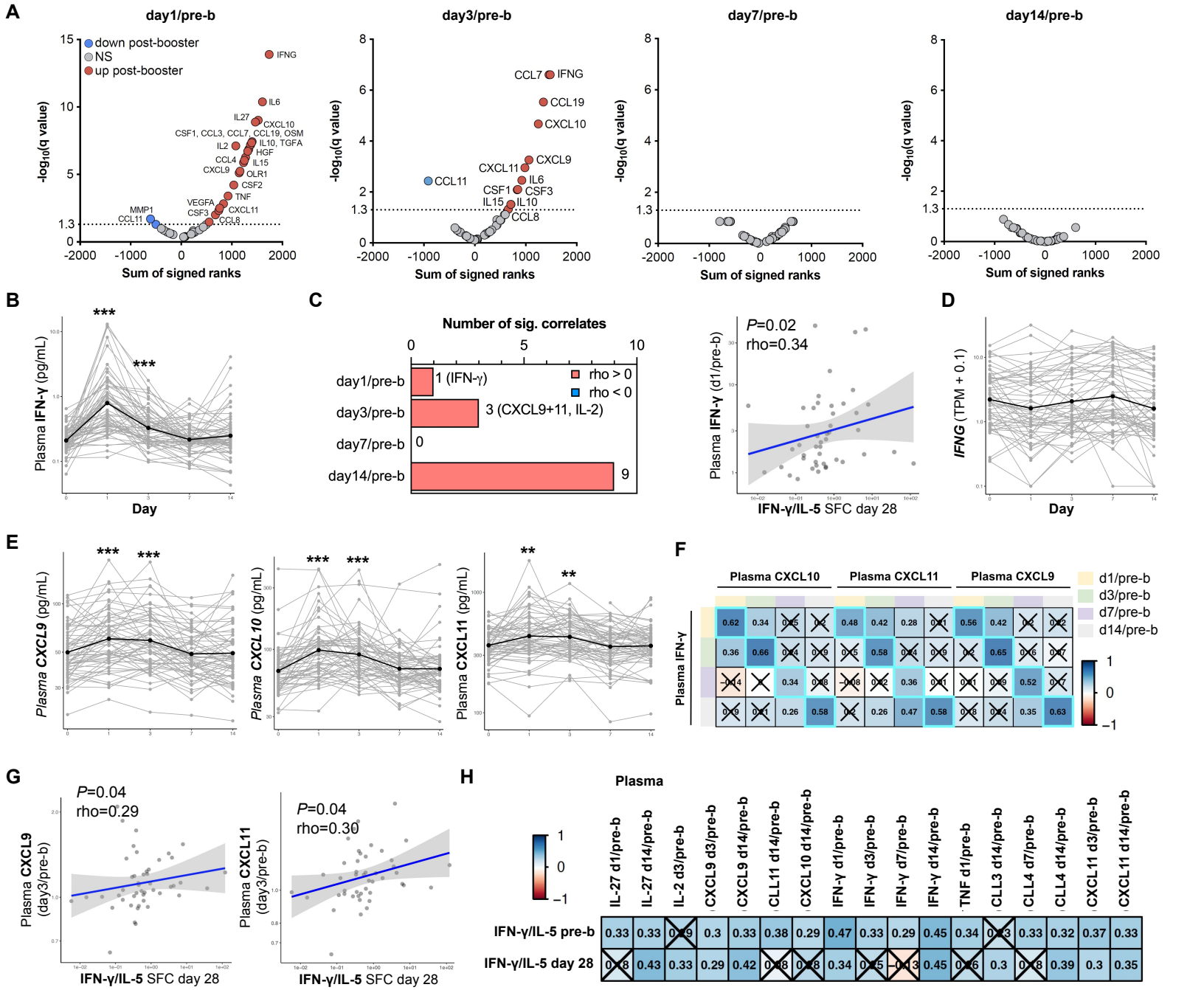

Figure 3. **Plasma IFN-γ concentrations increase after booster vaccination and its changes together with IFN-γ initiated cytokines enclose a positive association with Th1 polarization.**

A) Volcano plots showing the plasma cytokine concentration changes of day 1, 3, 7, 14 post/pre-booster vaccination with the sum of signed ranks of the Wicoxon matched-paired signed rank test (x-axis) and -$\log_{10}$(q-value) on the y-axis. Cytokines that are significantly increased and decreased are highlighted in red and blue respectively (q-value<0.05). **B**) Plasma concentrations of IFN-γ (pg/mL) over time. **C)** Number of significant Spearman correlations (*P*<0.05) of plasma cytokine changes vs T cell polarization 28 days post booster (IFN-γ/IL-5 SFC) and correlation between IFN-γ (day1/pre-b) and T cell polarization 28 days post booster (IFN-γ/IL-5 SFC). **D)** IFNG gene expression (TPM +0.1) over time with the black line indicating the mean expression. **E**) Plasma concentrations of CXCL9, CXCL10, and CXCL11 over time. **F**) Heatmap depicting Spearman correlation rho's of selected plasma cytokine changes showing that the dynamics of CXCL9-11 change with that of IFN-γ Insignificant correlates are crossed (*P*>0.05). **G**) *S*pearman correlation between either plasma CXCL9 (day3/pre-b) or CXCL11 (day3/pre-b) and T cell polarization data 28 days post booster (IFN-γ/IL-5 SFC). **H**) Heatmap depicting Spearman correlation rho's of selected plasma cytokine changes post/pre-b booster vaccination (columns) vs T cell polarization data before and after booster (rows). Insignificant results are crossed (*P*>0.05). Plasma cytokine n=59-61, RNA n=56, correlation analysis n=38-47. ***q-value<0.001, **q-value<0.01.

Figure 4

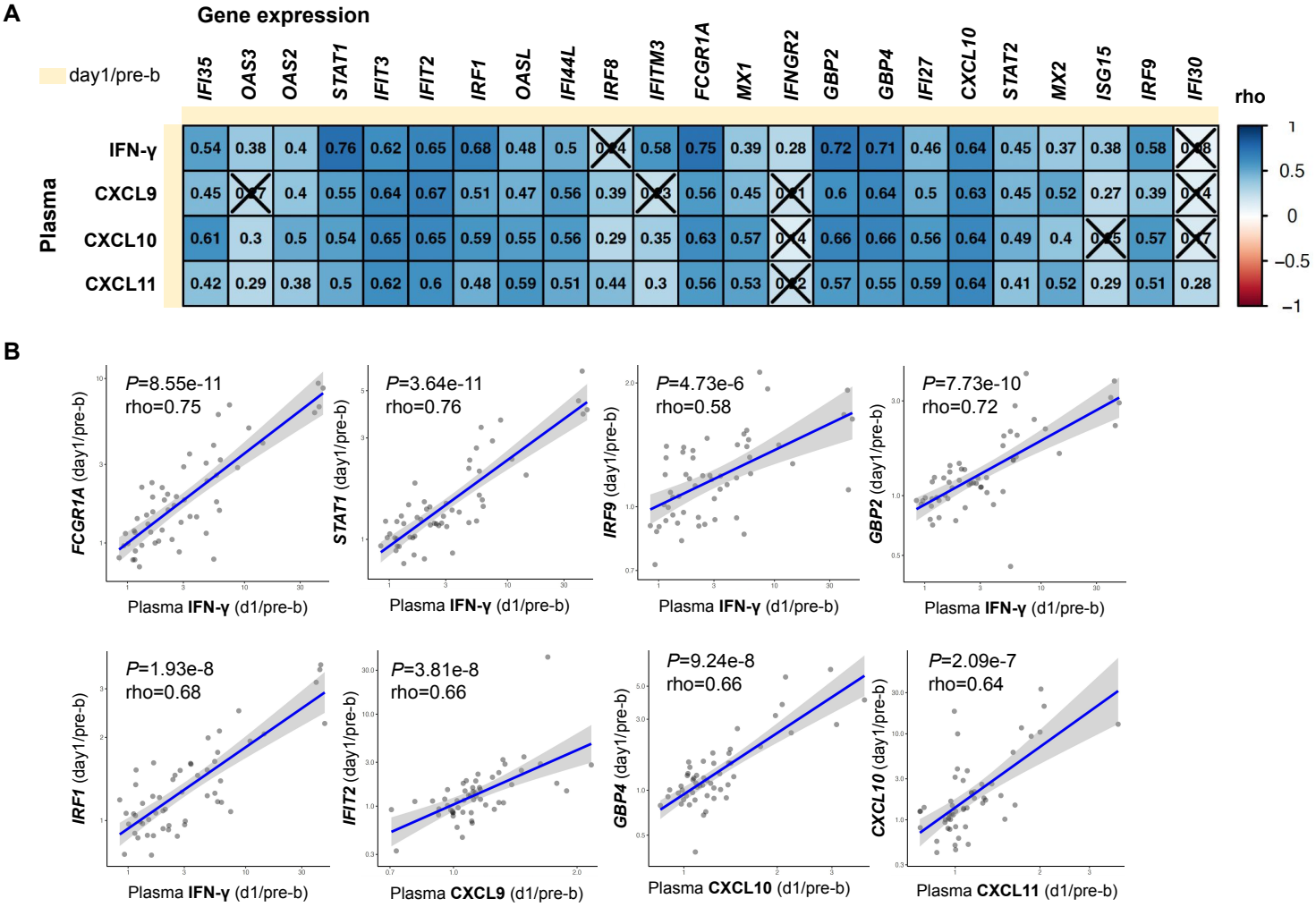

Figure 4. **Changes in plasma IFN-γ correlate with the magnitude of IFN response gene expression in PBMC and plasma cytokines.**

A) Heatmap depicting Spearman correlation rho's of selected plasma cytokine changes with vaccine-induced genes d1/pre-b (DEG). Insignificant correlates are crossed (*P*>0.05). **B**) Spearman correlation between either plasma IFN-γ, CXCL9-11 (day1/pre-b) and selected IFN and vaccine-induced genes d1/pre-b (DEG).

Graphical Abstract

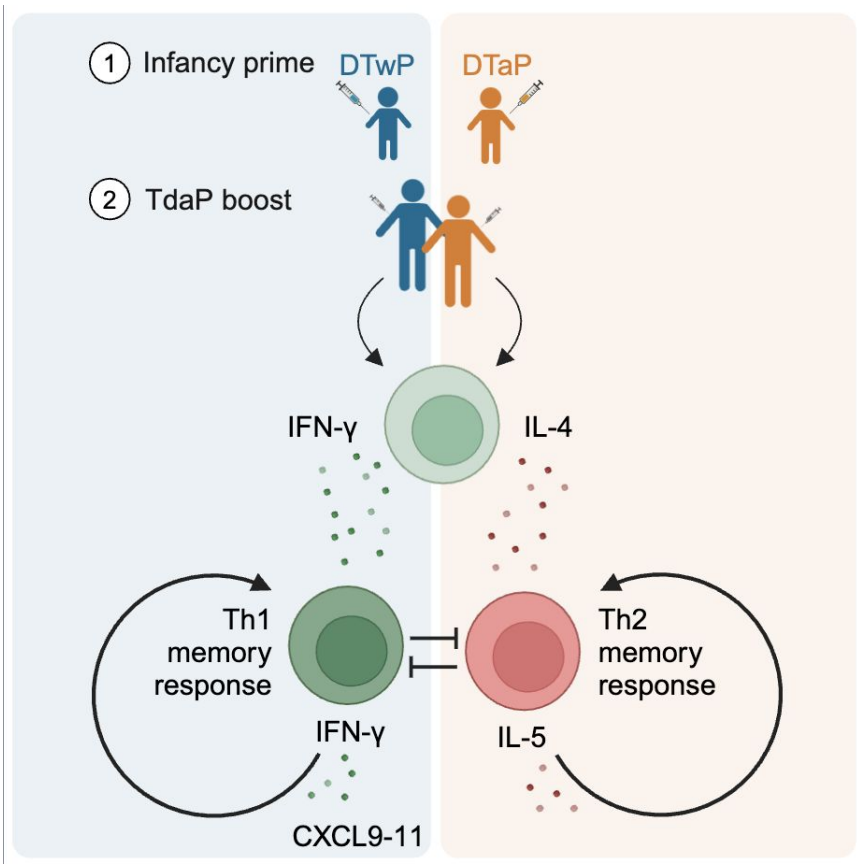

Figure S1

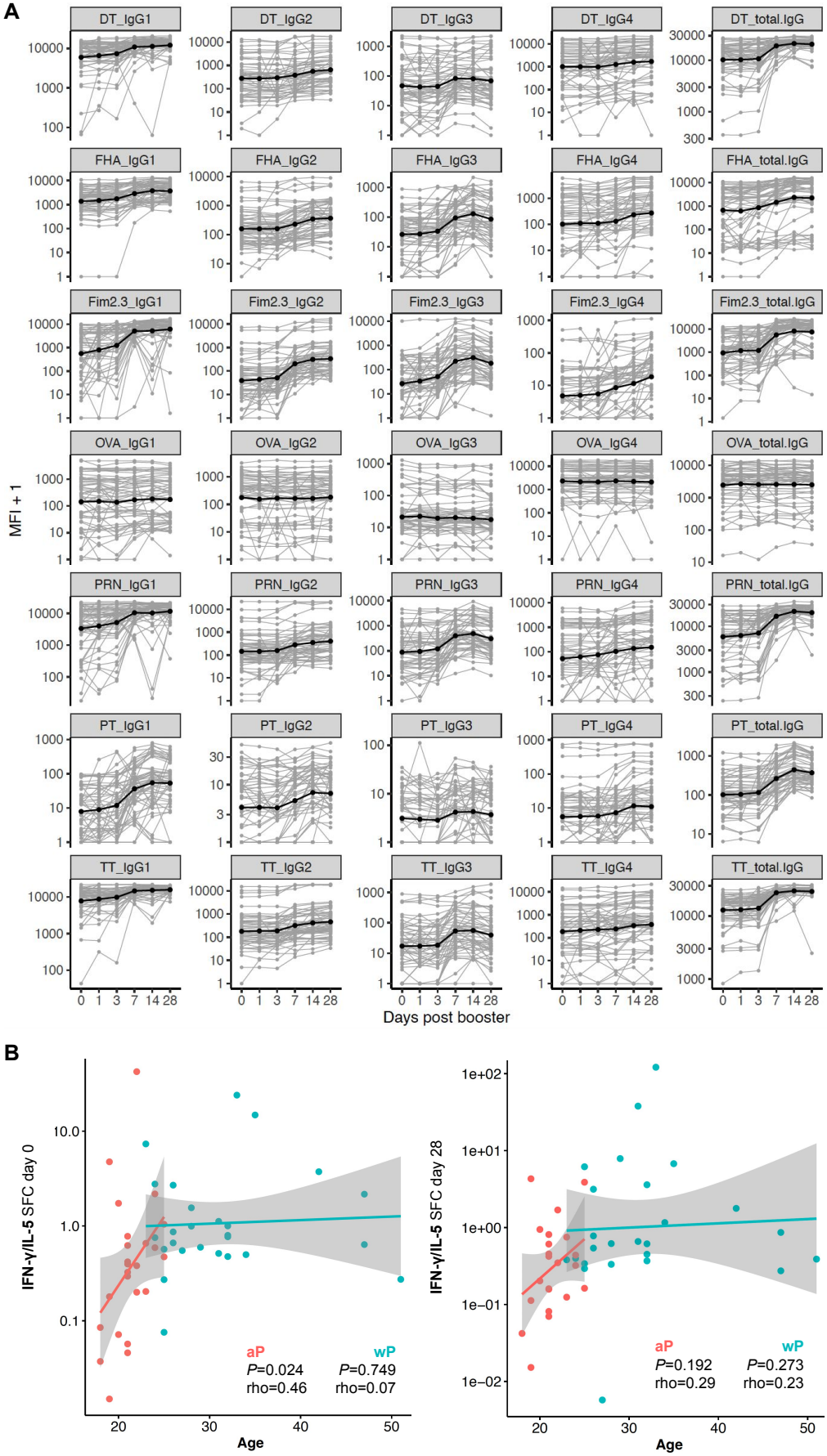

Figure S1. **A)** Plasma IgG measurements before and after Tdap booster vaccination. Shown are $\log_{10}$-scaled median fluorescence intensities (MFI) of IgG1-4 and total IgG against Tdap antigens (PT, PRN, FHA, FIM2/3, TT, and DT) and the non-Tdap antigen ovalbumin (OVA) for each participant (n=57) and time point (grey). The black lines and points indicate the medians. **B)** Spearman correlations between age at booster and T cell polarization data before and 28 days post booster (IFN-γ/IL-5 SFC) per vaccination group.

Figure S2

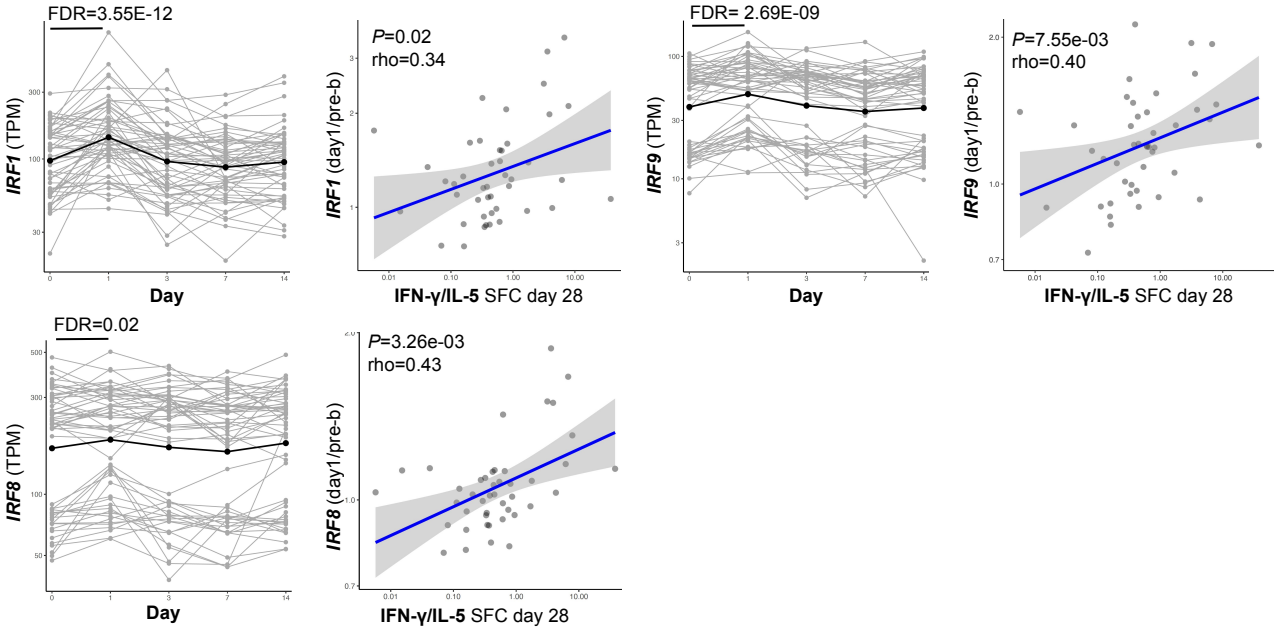

Figure S2. **Interferon signaling positively correlates with Th1 polarization.** *IRF1, IRF8* and *IRF9* gene expression (TPM) over time with the black line indicating mean expression and Spearman correlation between *IRF's* (day 1/pre-b) and T cell polarization data 28 days post booster (IFN-γ/IL-5 SFC). RNA n=56, correlation analysis n=44.

Figure S3

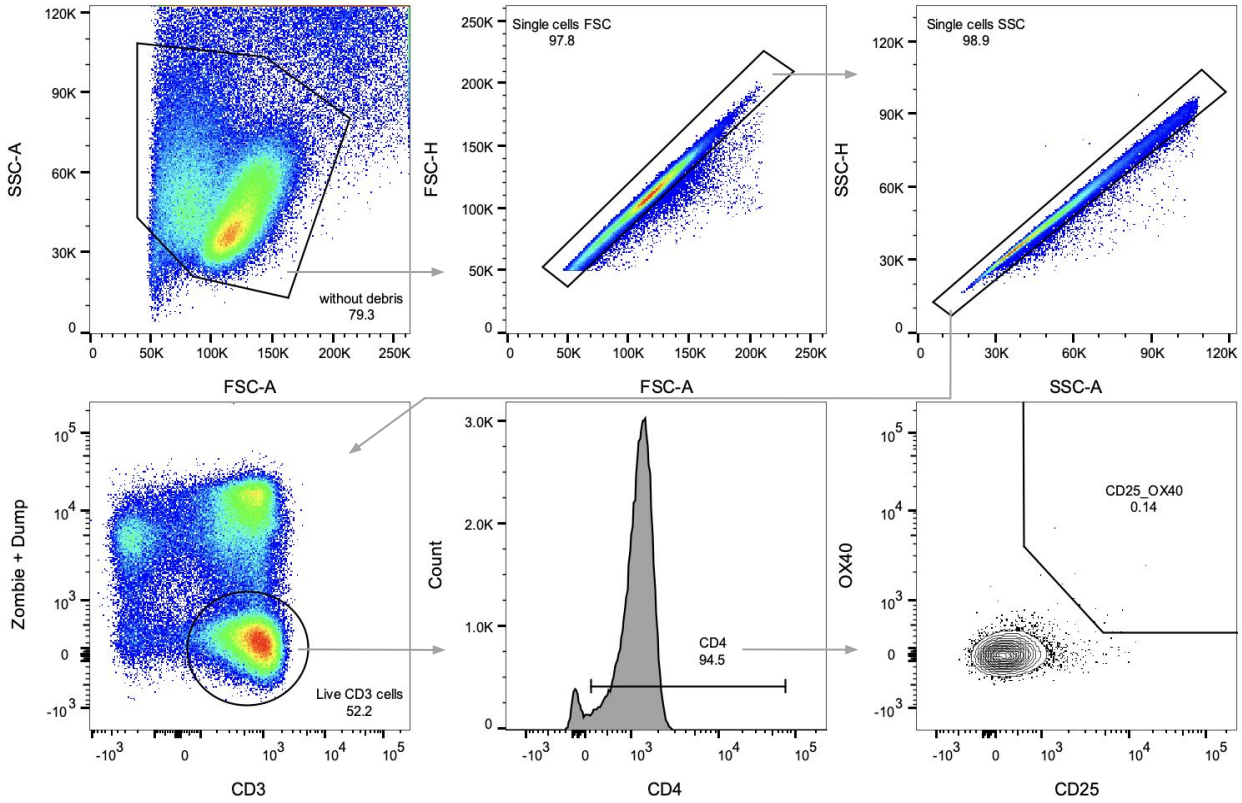

Figure S3. **Strategy for gating AIM CD25^{+}OX40^{+} CD4^{+} T cells.** The dump gate consisted of V500-conjugated CD8, CD14, and CD19.